Larhyss Journal, ISSN 1112-3680, n°59, Sept 2024, pp119-155

WATER DISTRIBUTION NETWORK LEAKAGE ANALYSIS USING WATERGEMS: A CASE STUDY FROM WESTMOORING, TRINIDAD AND TOBAGO

BANERJEE K.S.[1], MALLIKARJUNA V.[2], CHADEE A.A.[1], SMITH I.[1], LAKSHMIDEVI S.G.[3], SINGH, K.[4], PRASAD C.V.S.R.[5], AZAMATHULLA H.M.[1*]

[1] University of the West Indies, St Augustine, Trinidad
[2] V R Siddhartha Engineering College, Vijayawada, India
[3] Nalla Malla Reddy Engineering College, Narapally, Hyderabad, India
[4] Department of Computer Science Engineering, Rajkiya Engineering College, Sonbhadra, U.P., India
[5] Malla Reddy Engineering College, Secunderabad, India.

(*) Hazi.azamathulla@sta.uwi.edu

Research Article – Available at http://larhyss.net/ojs/index.php/larhyss/index
Received January 2, 2024, Received in revised form July 25, 2024, Accepted July 30, 2024

ABSTRACT

Water distribution is a critical system that involves engineered hydrologic and hydraulic components to provide water supply to a continuously growing population. Ensuring a sufficient and uniform water supply through a well-designed network is essential to meet the increasing water demand. The present study focuses on analyzing the water demand of the public water supply to facilitate effective planning, development, and operation of water supply and distribution networks. The main objective of the study is to analyze the existing water distribution network at West Moorings using the Watergems Software. To conduct this analysis, various data points are needed, such as the population of the area, water demand, distribution network layout, and water pump information. Additionally, details regarding the length, nodes, and diameter of the pipes are essential for the analysis. These data are input into the Watergems Software to perform analyses related to pressure, head loss, and elevation. The results of the analysis provide valuable information on pressure and flowrate at different nodes and head loss along various pipes in the network. By comparing the results obtained from the Watergems Software with actual data, the study aims to locate the leaks within the water distribution network at Westmooring, Trinidad and Tobago. In conclusion, Watergems identified leakage nodes within the West Moorings Network, and data analysis helped narrow down the leak's location in the field. This process involved model calibration using field pressure and flowrate data from WASA, and emitter coefficients were categorized by the Darwin Calibrator function. Accurate boundary inputs, such as the number of leakage

nodes, Initial Emitter Coefficient Spacing, and time intervals, were essential for precise data assumptions.

Keywords: Water Distribution, Watergems, Water Demand Analysis, Distribution Network, Westmooring.

INTRODUCTION

All living things require water for a variety of functions, including drinking, food preparation, irrigation, and manufacturing (Aroua, 2023; Rouissat and Smail, 2023). Less than 1% of the water on Earth is accessible as fresh water, and although though it makes up over 70% of the planet's surface, its distribution is not uniform across the planet (Peslier et al., 2017; Ihsan and Derosya, 2024). As a result, over a billion people, mostly in developing countries, do not have access to clean drinking water (Derdour et al., 2022). There are several obstacles to overcome worldwide to guarantee a safe, adequate, and dependable water supply (Berrezel et al., 2023; Kouloughli and Telli, 2023; Pandey et al., 2022).

Water distribution networks (WDN) are one of the most important parts of the water production network in a country or a region (Campisano and Modica, 2015; Dringoli, J., 2016; Fontana et al, 2016; Beker and Kansal, 2019; Patel and Mehta, 2022; Mehta et al., 2024). The water that it provides is important to the domestic, agricultural, and industrial facets of society (Hountondji and Codo, 2019; Kezzar and Souar, 2024). Concrete service reservoirs serve as backup supplies, while water towers can replace them in flat areas. Distribution mainly involves underground pipes to houses and establishments. Urban water supply faces challenges such as per capita disparities, inadequate monitoring of water quality, and reliance on distant sources for transportation (Aroua, 2022).

Leak detection is important to sustain a reliable water supply as stated by Modica (2015). Multiple articles went through many different methods of detecting leaks before they occurred (Dipali Babubhai Paneria, 2017). The numerous optimization methods are used in the identification of leaks in WDN, however, WaterGEMS (Water Geospatial Engineering Modeling System) software is widely used to detect and locate leaks present throughout the water network (Azadeh et al, 2013; Świtnicka et al., 2017; Salunke et al, 2018; Channel, 2019; Desta et al., 2022; Kowalka et al., 2022; Mohseni et al., 2022; Shahosseini et al, 2023).

WHY WEST MOORINGS?

Current project has analyzed the water distribution network at West Moorings, in Trinidad and Tobago using a Water Distribution Network (WDN) model to identify leaks by comparing model and field data. The aim is to enhance water quantity distribution to consumers. The scope includes collecting pipe and junction reports, analyzing the data with Bentley Watergems Software software, and comparing the results with actual data.

STUDY AREA AND DATA COLLECTION

Study Area

Westmoorings is a residential area located in the region of Diego Martin on the island of Trinidad, situated to the west of Port of Spain, the capital of Trinidad and Tobago. This area is nestled between the Gulf of Paria and the Diego Martin River, offering scenic views and convenient access to natural water bodies. The suburb caters to a wide demographic, ranging from lower middle-class to upper-class families, and is renowned throughout the country for its luxurious housing and significant expatriate population. The residential options in Westmoorings are diverse, featuring small apartments for more modest living arrangements and large upscale houses for those seeking a more opulent lifestyle. This blend of housing options contributes to its reputation as an upscale and desirable community.

Figure 1: Map Showing the West Moorings Area Source: (Google Earth)

Model Building

Before the analysis of the West Moorings Water Distribution system could be conducted, we first needed to build the model of the network. The entire network could not be built due to the Bentley Student Version having a limit on the total amount of pipes that can be modeled.

The Model was built using both Watergems from Bentley and Arc-Gis. Arc Gis was used to obtain the necessary geo spatial data of the network, ie: junction elevations throughout the network. Data of the network was provided which included a map of the network (including junction types and pipe sizes), commercial demand values and DMA data (i.e. Flowrate and pressure data). WaterGEMS software was used to input the pipe characteristics, junction types and characteristics. The Customer Meters nodes were used to represent the 10 commercial businesses present within the network that we have data for. Since we do not have a fully detailed map of the chosen study area, we assumed the pipe locations and sizing. Also, the junctions present within the area were determined by conducting a visit to the South East side of West Moorings area.

Figure 2: Image 2 Showing the Water network modeled in Watergems

Determining Flow

To simulate the pipe flow from the main Distribution 400mm Cast Iron line we used the reservoir and pump nodes methods as recommended by Watergems. The demand flowrate for the entire area of West Moorings was calculated by summing the average flowrate values for the commercial structures and the calculated flowrate of the residential area.

To obtain the residential demand data a current map of the area was used to determine the number of residential homes within the area, it was determined that there were approximately 180 homes within the area. it was assumed that each home was a 5-person dwelling. The residential demand calculations are seen below:

Q per household from WASA=0.014 m^3/h

Q for all households = Q per household*no of homes *Avg no of people living in dwelling

$$= 0.014*180*5$$

$$= 12.6\frac{m^3}{h} = 13\frac{m^3}{h}$$

The Fire Flow per hydrant was found to be 2275 l/d = 0.01 m^3/h. there are six hydrants on the system therefore fire flow = 0.06 m^3/h.

The data for the International School of Port of Spain and La Riviera Apartment complex was unavailable so we used the data from the WASA guidelines for the average usage of a school and household to determine their demands.

School Day with Cafeteria, gym and Showers = 95l/d = 0.004m^3/h

The School Population is 257 according to there site.

School Water Demand=257*0.004=1.028 m^3/h

Residential Structures 350 l/d= 0.014 m^3/h

Total Number of apartments within La Riviera = 96

$$= 0.014 * 96 = 1.344\frac{m^3}{h}$$

The total flowrate of the commercial buildings data in the area is 16.19 $\frac{m^3}{h}$ =17 $\frac{m^3}{h}$ therefore the total for the entire area is 30 $\frac{m^3}{h}$.

The pump head was determined using the equation,

$H = z + H_f$

where:

z is the difference in height between the pump and the highest point in West Moorings

H_f = Head Loss per 100m

Z = 2.3 - 0.04 = 2.26m

h_f was found using the friction loss Charts from the image num from the appendix = 0.98

The Total Length of the network was obtained from Watergems Flex Tables for Pipes, it was determined to be 5522m. m per 100m $\frac{5522}{100} = 55.22$

H_f = 0.98*55.22

= 54.12m

$\therefore H = 2.26 + 54.12 = 56.38m$

The Customer Meter Node function was used to represent the commercial structures within the model and allowed for the individual demand values to be inputted into the model. We connected the meter to the junctions using the lateral pipe function.

After building the model, the initial analysis of the system was conducted to determine the model flowrates and pressures. The Analysis method used was the Extended period simulation for a 24-hour period at 30-minute intervals. The demand values at the customer meters were multiplied by a multiplier factor to simulate the real-world flow conditions at a school, commercial centers and residential homes for a 24 hour period. Fig. 3 represents the flowrates obtained at pipe 393, while Fig. 4 shows the comparison between Field Flowrate and Model Flowrate.

Figure 3: Flowrate vs Time @ P-393

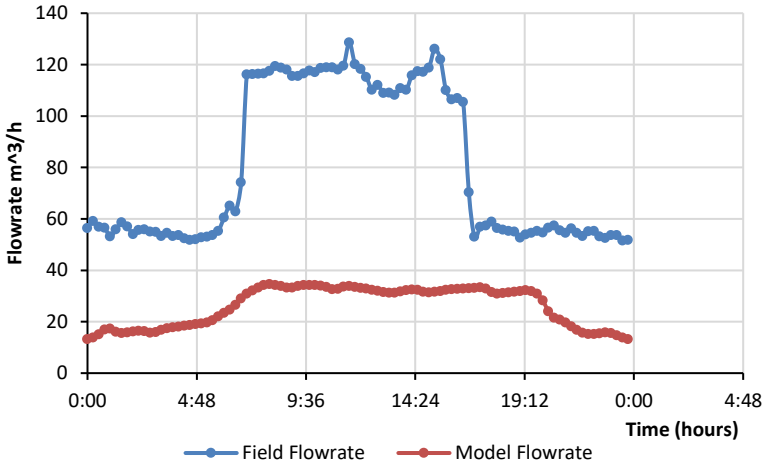

Figure 4: Comparison between Field Flowrate and Model Flowrate

NB: since the project area (West Moorings) cannot be modeled in watergems due to student access limitations the demands shown are not accurate. Normally a discrepancy like the one above will be present until the graph is calibrated using the Darwin Calibrator.

Darwin Calibrator

To conduct a leakage analysis, we used the Darwin Calibrator Function within Watergems. This calibration is done using the genetic algorithms which makes up the basis of the software function. We first created a new calibration study. Then data was inputted into the software for a 24-hour period at 15-minute intervals as shown below. At each interval we looked at the flowrate ($\frac{m^3}{h}$) and pressure (psi) at Pipe 377 and Junction 344 respectively. The images 1 and 2 below show the Calibrator Window and inputted DMA data. Fig. 5 shows Pipe 377 and Junction 344.

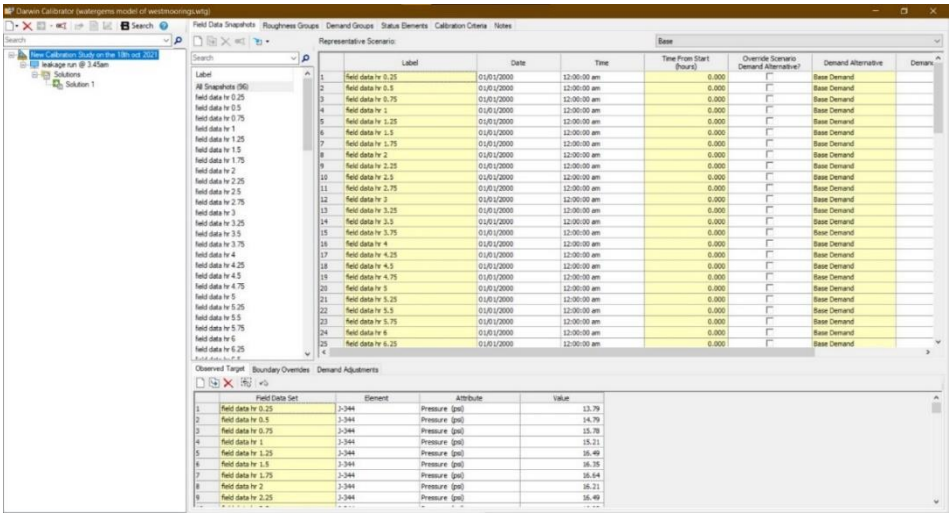

Image 1: Image Showing Darwin Calibrator window with DMA data for a 24 hour

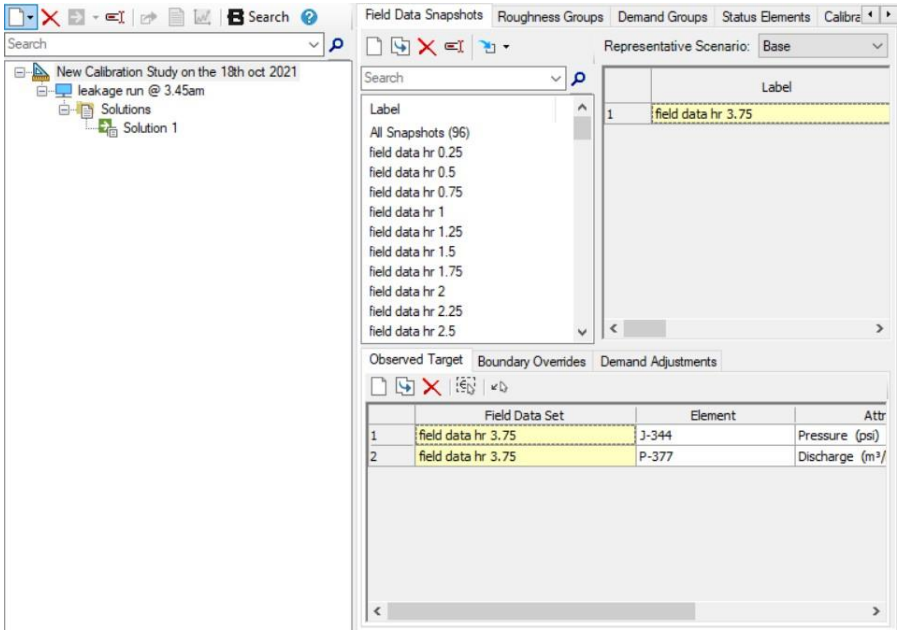

Image 2: Showing Darwin Calibrator window with 3:45am Pressure and Flowrate Data Highlighted

Figure 5: Pipe 377 and Junction 344

The data within the above images represents the flowrate and pressure for the 18th of October 2021. The other dates we will be looking at are 17th and 19th of October 2021.

Next an Optimized Run for the field data @ 3am was created, and we specified detect leakage node in the Operation Column. Then the minimum and maximum emitter coefficients and their spacing were stated. This process was repeated @ 1am, 2am, 4am and the period between 1-4am to determine if the leaks viewed at 3am were the same. The test is done when customer water usage is very low to ensure accurate results. Images 3 and 4 below show the process within the Darwin Calibrator.

Image 3: Showing the Optimized run: Emitter Coefficient's Max=1, Min=0 and at a spacing of 0.1

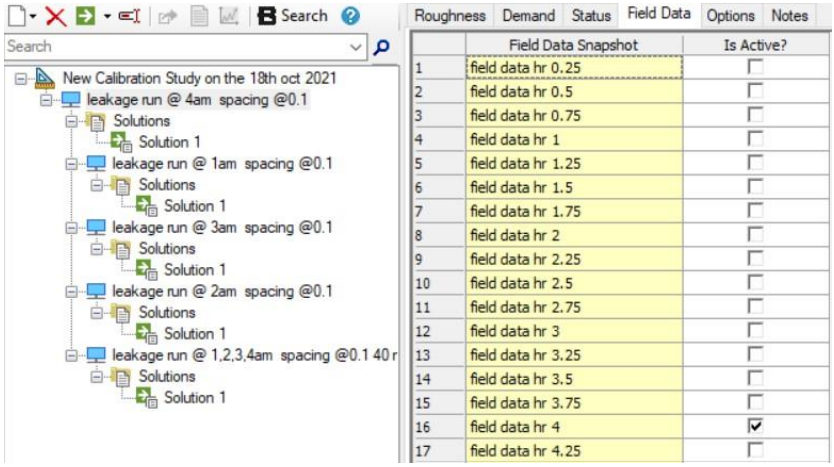

Image 4: Showing The Optimized Run, field data screen.

Leak Identification

A key for the Emitter Coefficient in the junctions and Pressure Loss within the pipes was created to easily identify the junctions and pipes on the system where there are possible leaks (Images 5 and 6).

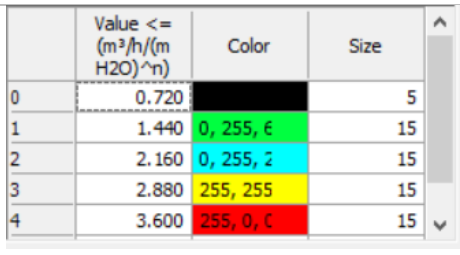

Image 5: Showing Emitter Coefficient Key.

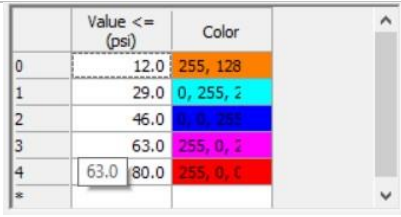

Image 6: Showing Pressure Key.

RESULTS AND DISCUSSION

The New Emitter Coefficients for the junctions are obtained when we used the DMA data for a 1 hour period in the Darwin Calibrator. After exporting the new values into the model as its own scenario we identified the general locations of leaks within the network.

NB: the highlighted junctions are not the exact leak locations they show the general area within the system where leaks are present.

The group of tables show the Emitter Coefficient values and the Flowrate values at the respective junctions for the 18th and 17th of October 2021 @ 1am, 2am, 3am 4am and between the hours of 1am and 4am.

Firstly, we determined that using a large number of leakage nodes was necessary to obtain multiple data points which can be used to narrow down the leak junctions within the model. The spacing of the Emitter Coefficient was another factor looked at. The smaller spacing allowed for increase precision in determining the emitter coefficients at the leakage nodes.

The first two tables show that the smaller Emitter Coefficient value provides a large number of leakage nodes. Therefore, for the rest of the analysis we will use 0.0036 $\frac{m^3/h}{(m\ per\ H_2O)^n}$ to identify the leakage nodes. The smaller value also gives a more precise Emitter Coefficient value which will further help with classifying the faults within the system.

This value is used by watergems to determine the Flowrate at the junctions highlighted to create the graphs for comparison of flowrate between the model data and the leakage run values. This can be further used to determining the average volume of water lost within that period. Flowrate is determined in WaterGEMS using the equation below:

$$Q = KP^n$$

$$where:\ K = Emitter\ Coefficient\ @junction\left(\frac{\frac{m^3}{h}}{(m\ per\ H_2O)^n}\right)$$

$P = Pressure\ Head\ (m)@\ the\ junction$.

The Pressure at the junction is obtained from the properties tab of the software.

$n = Pressure\ exponent\ for\ orifice\ is$ 0.5

Table 1-6 Shows the data collected for the period of 1-4am and individual time intervals of 1,2,3 and 4 am. The individual time intervals show a correlation between one another but there is multiple sets of data that vary. Therefore, it was determined that using the period of 1-4 am when calibrating would be more accurate when conducting a leakage analysis.

Table 1: Showing the Emitter Coefficient Data from WaterGEMS @ 2am on the 18th OCT 2021

Time: 2am	0< Emitter Coefficient <3.6	Number of leakage Nodes: 40	Emitter Coefficient Spacing 0.036
Junction	**Emitter Coefficient**	**Demand m^3/h**	
J-317	3.600	8.118	**Image 10 Showing the leaks present on the network**
J-350	3.600	6.378	
J-393	3.384	6.004	
J-337	2.880	5.637	10 points > 0
J-397	2.880	6.717	
J-332	1.404	2.842	
J-394	0.828	1.467	
J-352	0.792	3.645	
J-324	0.540	1.056	
J-335	0.468	3.088	
J-32	0.000	0.000	

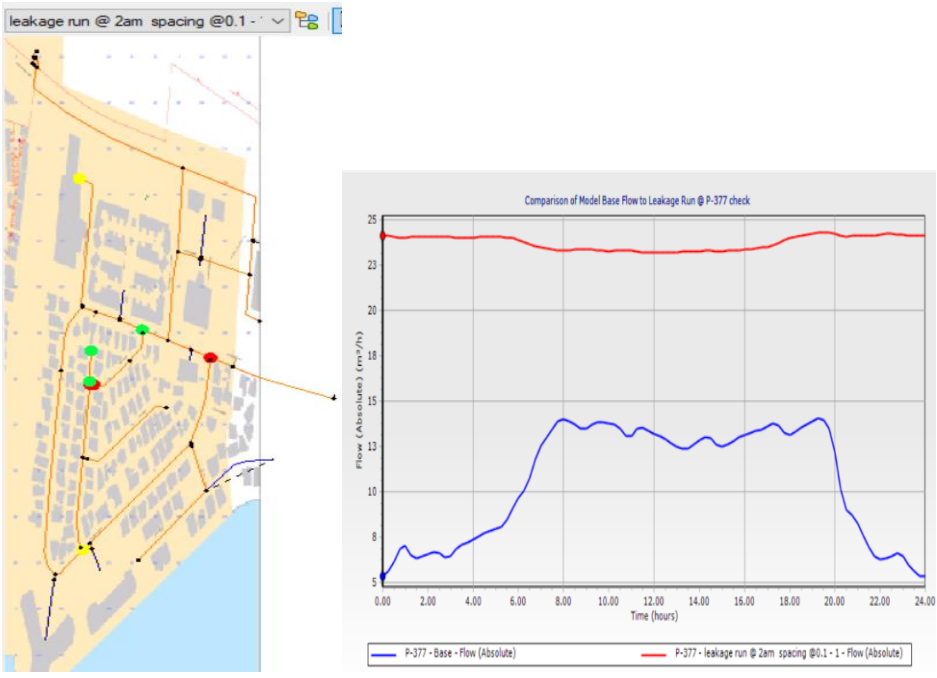

Figure 6: Graph Showing Comparison of Model Base Flow to Leakage Run @ P-377 check

Table 2: Showing the Emitter Coefficient Data From WaterGEMS @ 2am on the 18th OCT 2021

Time: 2am	0< Emitter Coefficient <3.6	Number of leakage Nodes: 40	Emitter Coefficient Spacing 0.0036
Junction	**Emitter Coefficient**	**Demand m^3/h**	
J-322	3.445	8.965	**Image 11 Showing the leaks present on the network**
J-334	3.053	5.285	
J-350	2.578	4.548	
J-392	2.225	3.847	
J-400	2.207	4.465	15 points > 0
J-352	1.559	5.073	
J-408	1.483	3.319	
J-318	1.181	2.448	
J-337	1.127	2.167	
J-414	0.673	1.394	
J-117	0.670	1.428	
J-335	0.396	2.928	
J-395	0.248	0.832	
J-387	0.076	1.061	
J-332	0.011	0.053	
J-32	0.000	0.000	

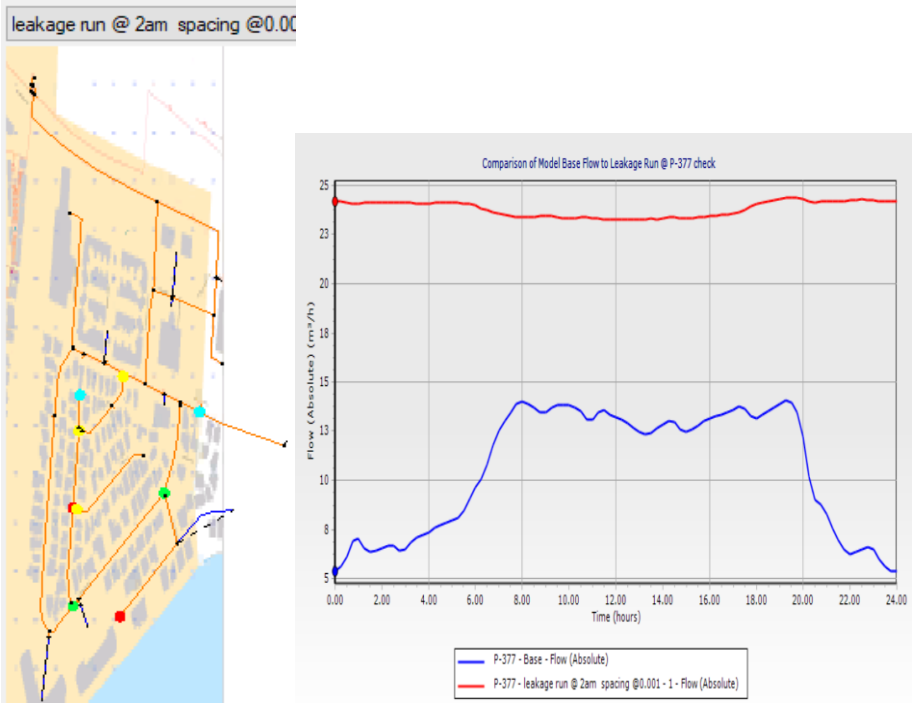

Figure 7: Graph Showing Comparison of Model Base Flow to Leakage Run @ P-377 check on the 18th OCT 2021

The data for the 18th of October 2021 is shown below.

Table 3: Showing the Emitter Coefficient Data From WaterGEMS @ 1am on the 18th OCT 2021

Time: 1am	0< Emitter Coefficient <3.6	Number of leakage Nodes: 40	Emitter Coefficient Spacing 0.0036
Junction	**Emitter Coefficient**	**Demand m^3/h**	
J-345	3.600	7.436	**Image 12 Showing the leaks present on the network**
J-334	3.053	4.978	
J-117	2.513	4.884	
J-121	2.225	4.493	17 points > 0
J-400	2.207	4.054	
J-387	1.919	4.592	
J-318	1.300	2.569	
J-408	0.907	1.853	
J-350	0.706	1.173	
J-414	0.666	1.264	
J-352	0.522	3.083	
J-335	0.396	2.894	
J-388	0.364	0.657	
J-332	0.356	0.657	
J-397	0.248	1.023	
J-343	0.220	0.773	
J-385	0.058	0.821	
J-32	0.000	0.000	

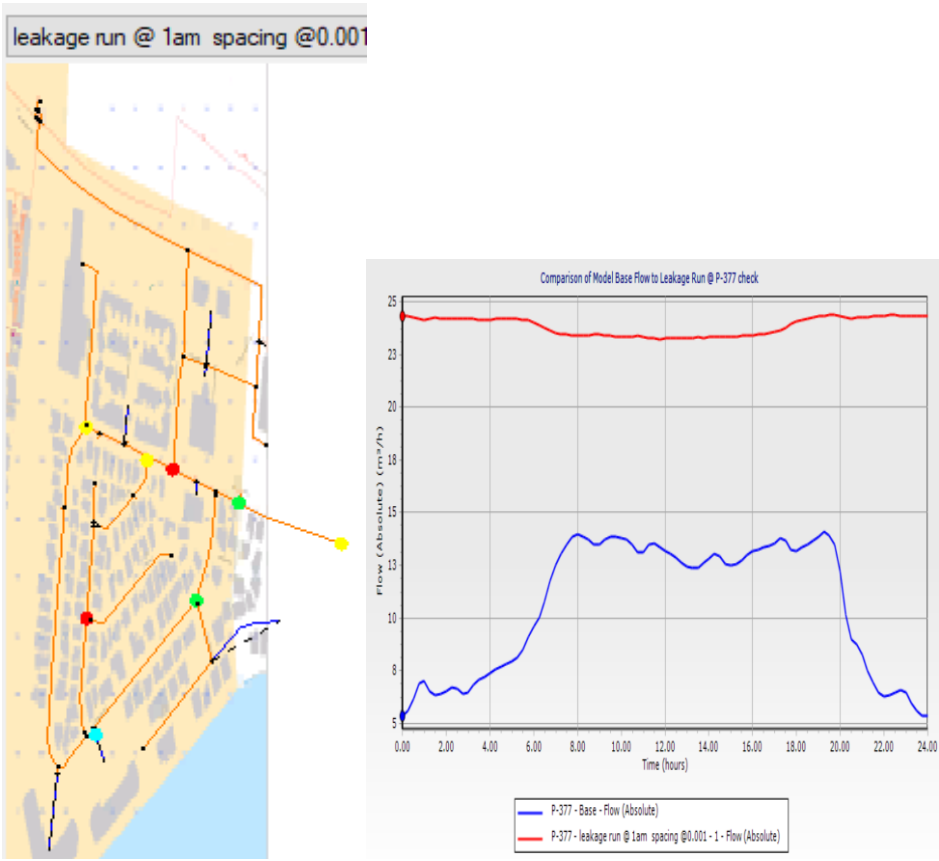

Figure 8: Graph Showing Comparison of Model Base Flow to Leakage Run @ P-377 check on the 18th OCT 2021

Table 4: Showing the Emitter Coefficient Data from WaterGEMS @ 3am on the 18th OCT 2021

Time: 3am	**0< Emitter Coefficient <3.6**	**Number of leakage Nodes: 40**	**Emitter Coefficient Spacing 0.0036**
Junction	**Emitter Coefficient**	**Demand m^3/h**	
J-408	3.442	6.279	**Image 13 Showing the leaks present on the network**
J-335	2.822	6.626	
J-350	2.578	3.528	
J-334	2.574	3.445	
J-410	2.545	3.819	16 points > 0
J-117	2.513	4.387	
J-318	2.365	4.145	
J-400	2.207	3.575	

J-121	2.196	3.935
J-414	0.666	1.126
J-387	0.421	1.624
J-337	0.313	0.492
J-332	0.259	0.423
J-395	0.248	0.727
J-385	0.094	0.833
J-344	0.004	0.051
J-32	0.000	0.000

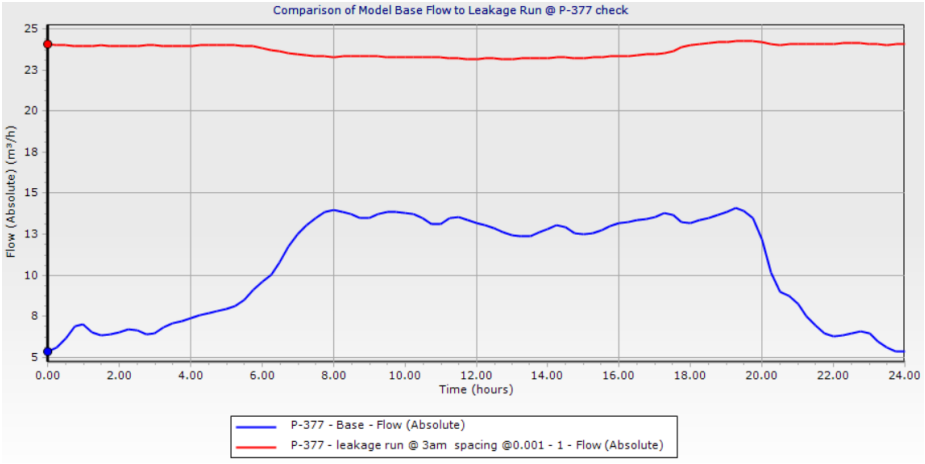

Figure 9: Graph Showing Comparison of Model Base Flow to Leakage Run @ P-377 check on the 18th OCT 2021

Table 5: Showing the Emitter Coefficient Data From WaterGEMS @ 4am on the 18th OCT 2021

Time: 4am	**0< Emitter Coefficient <3.6**	**Number of leakage Nodes: 40**	**Emitter Coefficient Spacing 0.0036**
Junction	**Emitter Coefficient**	**Demand m^3/h**	
J-322	3.388	8.557	**Image 14 Showing the leaks present on the network**
J-350	2.578	4.432	
J-341	2.545	4.861	
J-385	2.322	4.882	
J-117	2.052	4.174	16 points > 0
J-121	1.994	4.167	

J-408	1.829	3.832
J-318	1.152	2.283
J-345	1.127	2.447
J-414	0.673	1.328
J-352	0.637	3.322
J-335	0.288	2.706
J-395	0.248	0.809
J-338	0.083	0.150
J-332	0.004	0.050
J-32	0.000	0.000

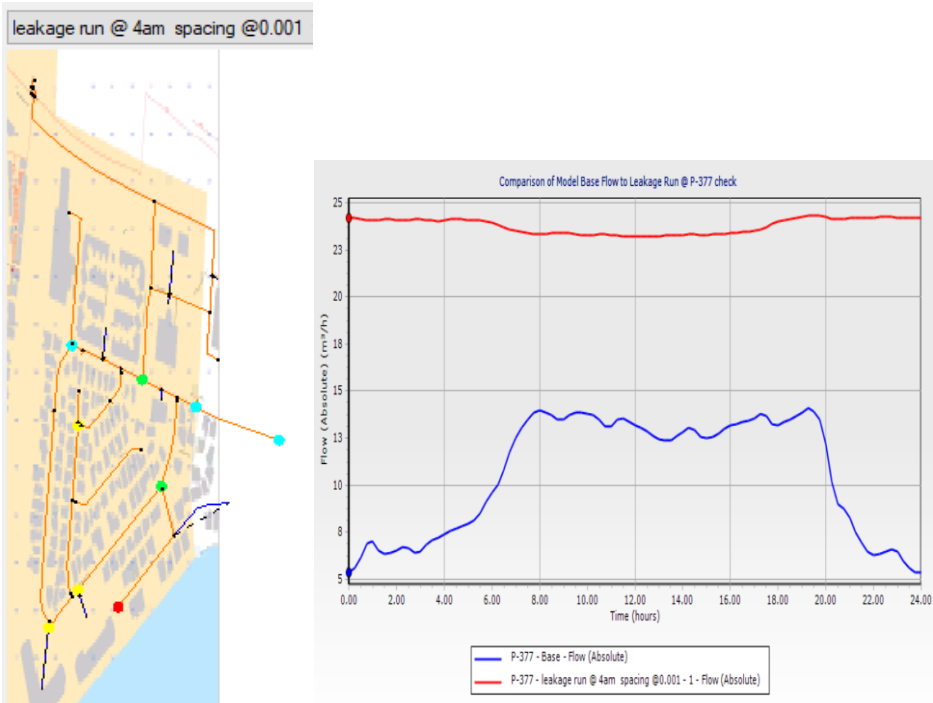

Figure 10: Graph Showing Comparison of Model Base Flow to Leakage Run @ P-377 check

Table 6: Showing the Emitter Coefficient Data From WaterGEMS @ 1-4am on the 18th OCT 2021

Time: 1-4am	0< Emitter Coefficient <3.6	Number of leakage Nodes: 40	Emitter Coefficient Spacing 0.0036
Junction	**Emitter Coefficient**	**Demand m^3/h**	**Image 15 Showing the leaks present on the network**
J-408	3.600	7.333	
J-334	3.053	4.724	
J-392	2.963	4.577	
J-350	2.578	4.084	15 points > 0
J-341	2.560	4.701	
J-400	2.207	4.025	
J-345	1.253	2.614	
J-117	1.098	2.138	
J-332	0.950	1.743	
J-414	0.673	1.272	
J-352	0.637	3.242	
J-335	0.396	2.865	
J-121	0.382	0.955	
J-395	0.248	0.781	
J-387	0.076	1.050	
J-385	0.058	0.792	
J-32	0.000	0.000	

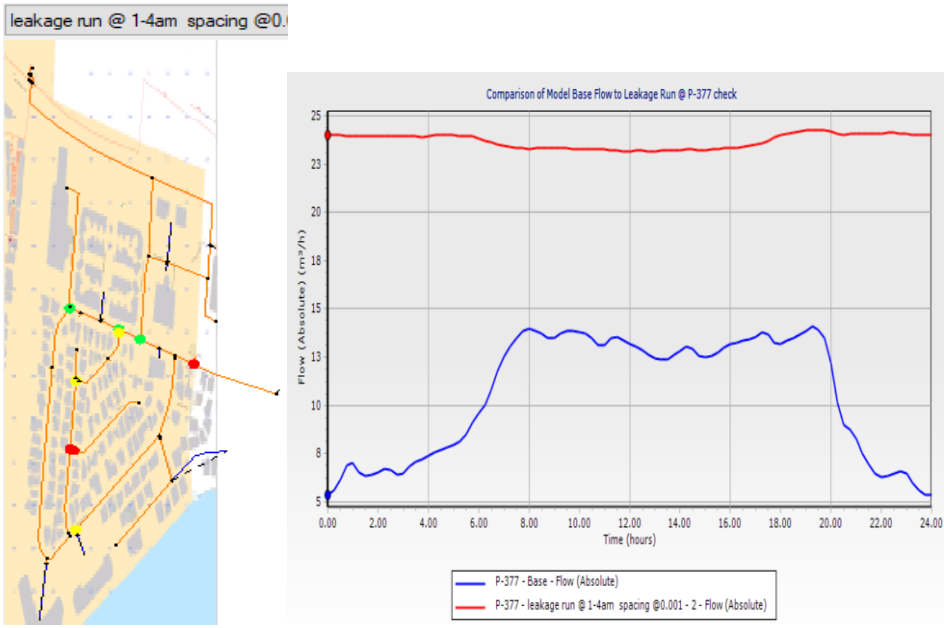

Figure 11: Graph Showing Comparison of Model Base Flow to Leakage Run @ P-377 check on the 18th OCT 2021

Table 7: Showing the Data from WaterGEMS @ 1-4am on the 18th OCT 2021

Time: 10-11:45pm	0< Emitter Coefficient <3.6	Number of leakage Nodes: 40	Emitter Coefficient Spacing 0.0036
Junction	**Emitter Coefficient**	**Demand m^3/h**	**Image 17 Showing the leaks present on the network**
J-412	3.571	4.117	
J-408	3.557	4.916	
J-322	3.445	6.368	
J-335	3.114	5.671	
J-350	2.578	1.988	17 points > 0
J-344	2.538	6.477	
J-117	2.513	3.155	
J-121	2.225	2.917	
J-400	2.214	2.415	
J-387	1.919	3.283	
J-332	1.181	1.298	
J-338	1.127	1.121	
J-380	0.817	2.383	
J-352	0.580	2.736	
J-414	0.558	0.666	
J-395	0.248	0.582	
J-385	0.058	0.759	
J-32	0.000	0.000	

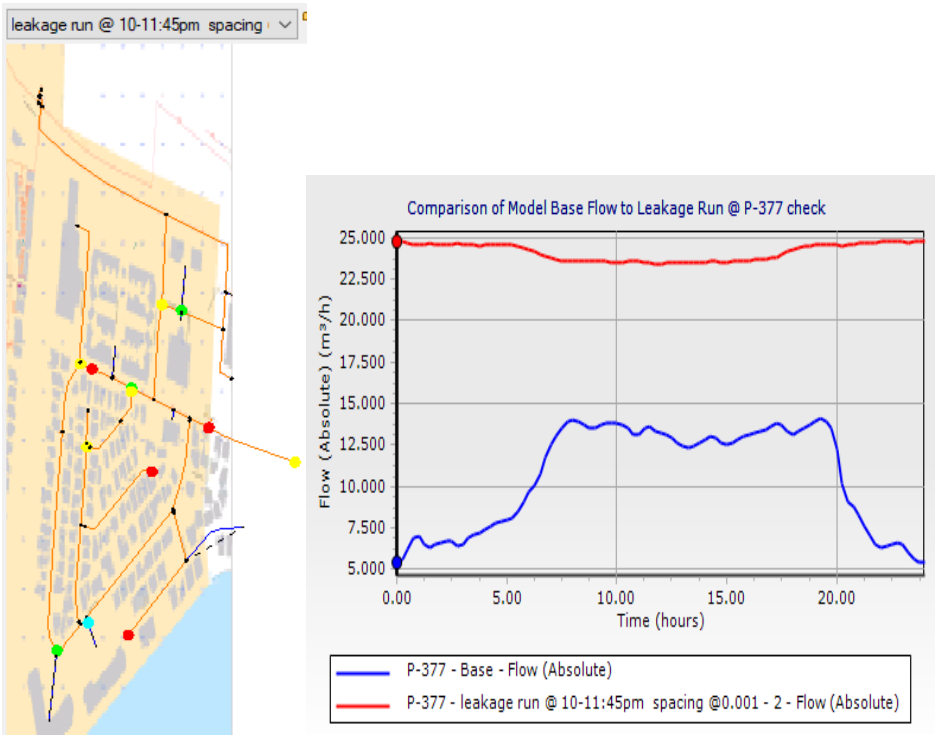

Figure 12: Graph showing Comparison of Model Base Flow to Leakage Run @ P-377 check on the 17th OCT 2021

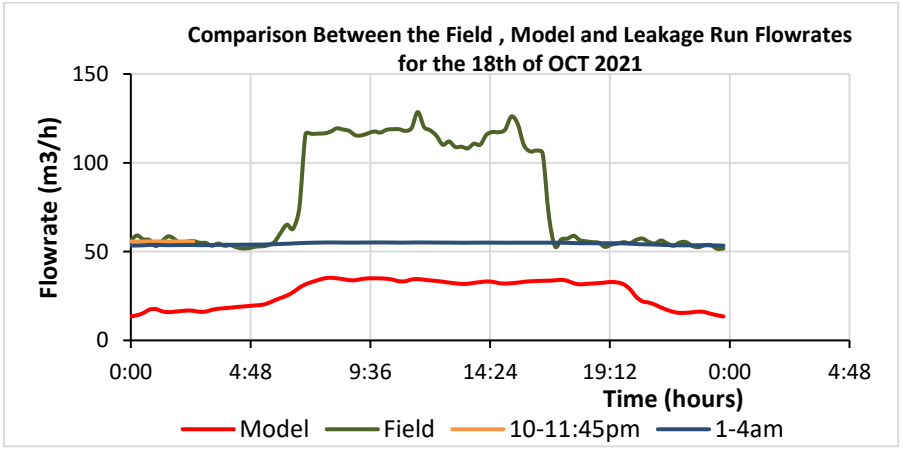

Figure 13: Graph showing the Comparison Between the leakage Runs, Base Model and Field Flowrates

The data for the 17th of October 2021 is shown below.

Table 8: Showing the Data from WaterGEMS @ 1-4am on the 17th OCT 2021

Time: 1-4am	**0< Emitter Coefficient <3.6**	**Number of leakage Nodes: 40**	**Emitter Coefficient Spacing 0.0036**
Junction	**Emitter Coefficient**	**Demand m^3/h**	
J-412	3.600	5.245	**Image 18 Showing the leaks present on the network**
J-334	3.575	3.796	
J-322	3.330	7.012	
J-350	2.578	2.923	
J-341	2.545	3.591	18 points > 0
J-392	2.225	2.358	
J-400	2.207	3.188	
J-375	2.012	3.088	
J-387	1.919	3.719	
J-390	1.253	2.188	
J-318	1.181	1.816	
J-345	1.098	1.971	
J-117	0.670	1.028	
J-352	0.637	2.984	
J-335	0.396	2.709	
J-395	0.245	0.669	
J-348	0.072	0.244	
J-385	0.058	0.770	
J-32	0.000	0.000	

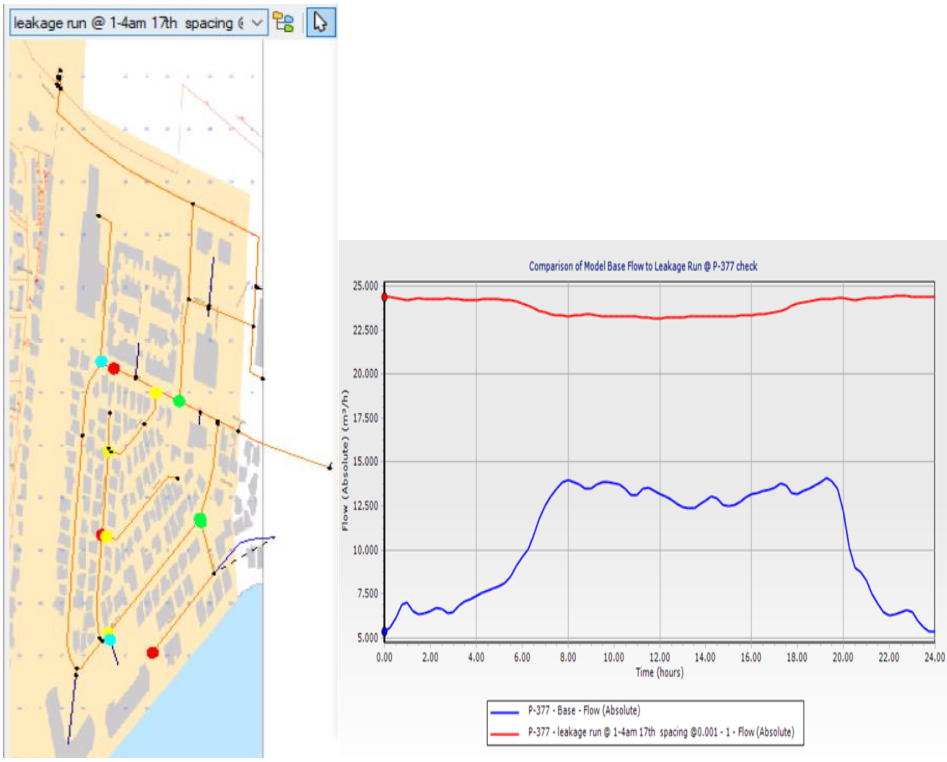

Figure 14: Graph Showing Comparison of Model Base Flow to Leakage Run @ P-377 check on the 17th OCT 2021

Table 9: Showing the Emitter Coefficient Data from WaterGEMS @ 10-11:45pm on the 17th OCT 2021

Time: 10-11:45pm	**0< Emitter Coefficient <3.6**	**Number of leakage Nodes: 40**	**Emitter Coefficient Spacing 0.0036**
Junction	**Emitter Coefficient**	**Demand m^3/h**	**Image 19Showing the leaks present on the network**
J-412	3.600	4.400	
J-350	3.499	2.651	
J-360	3.434	4.707	
J-334	3.341	2.227	
J-322	3.330	6.224	18 points > 0
J-392	2.963	1.961	
J-410	2.660	2.625	
J-341	2.538	2.912	
J-387	2.380	3.795	
J-400	2.207	2.544	

J-335	2.192	4.593
J-121	1.994	2.812
J-318	1.181	1.526
J-345	1.123	1.711
J-408	0.673	0.982
J-117	0.670	0.885
J-385	0.058	0.758
J-395	0.018	0.394
J-32	0.000	0.000

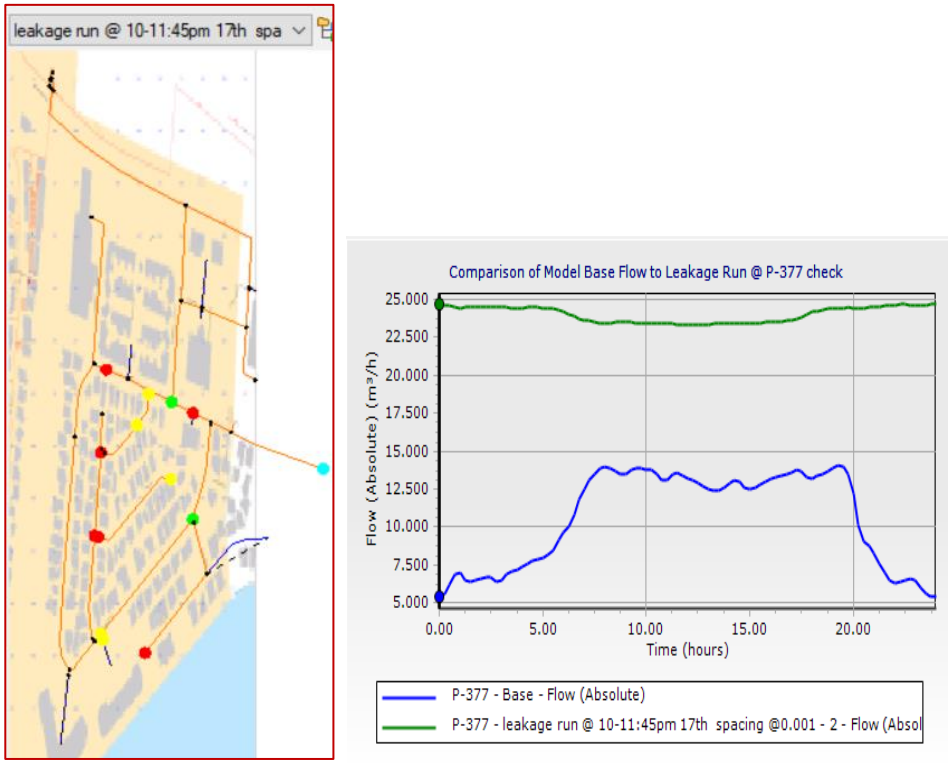

Figure 15: Graph showing Comparison of Model Base Flow to Leakage Run @ P-377 check on the 17th OCT 2021

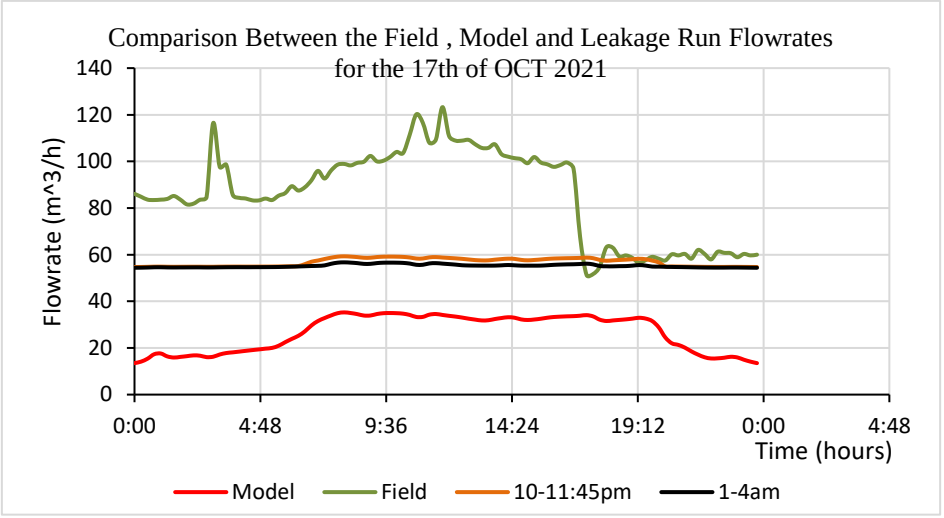

Figure 16: Graph showing the Comparison Between the leakage Runs, Base Model and Field Flowrates

The data below is for the 19th of October 2021.

Table 10: Showing the Emitter Coefficient Data from WaterGEMS @ 1-4am on the 19th OCT 2021

Time: 1-4am	0< Emitter Coefficient <3.6	Number of leakage Nodes: 40	Emitter Coefficient Spacing 0.0036
Junction	**Emitter Coefficient**	**Demand m^3/h**	
J-344	3.600	8.456	**Image 20 Showing the leaks present on the network**
J-412	3.600	3.605	
J-322	3.445	5.868	
J-334	3.341	1.171	
J-335	3.114	5.110	20 points > 0
J-392	2.963	1.015	
J-350	2.578	1.245	
J-341	2.545	2.525	
J-117	2.513	2.811	
J-121	2.225	2.709	
J-400	2.207	2.025	
J-387	1.919	2.958	
J-332	1.854	1.718	
J-318	1.181	1.354	
J-380	1.127	3.016	
J-408	0.673	0.875	

J-352	0.637	2.667
J-343	0.313	0.875
J-395	0.248	0.534
J-385	0.058	0.751
J-32	0.000	0.000

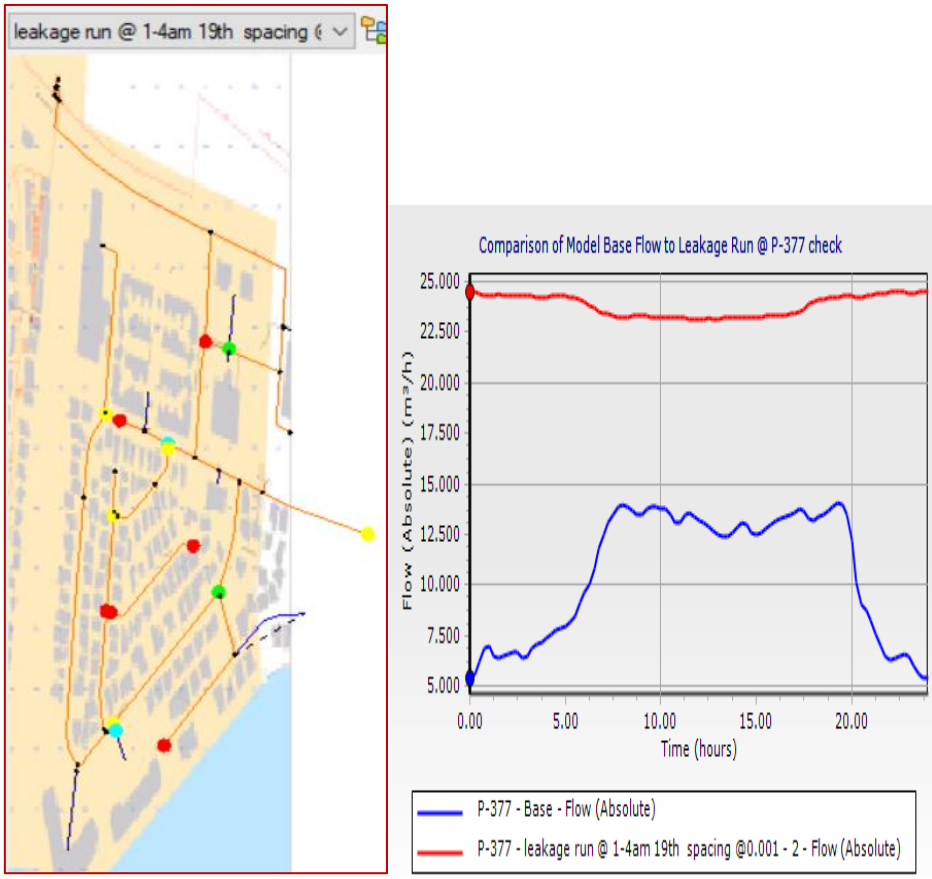

Figure 17: Graph showing Comparison of Model Base Flow to Leakage Run @ P-377 check on the 17th OCT 2021

Table 11: Showing the Data from WaterGEMS @ 10-11:45pm on the 19th OCT 2021

Time: 10-11:45pm	**0< Emitter Coefficient <3.6**	**Number of leakage Nodes: 40**	**Emitter Coefficient Spacing 0.0036**
Junction	**Emitter Coefficient**	**Demand m^3/h**	**Image 21 Showing the leaks present on the network**
J-334	3.341	4.542	
J-322	3.330	7.897	
J-335	3.053	7.020	
J-392	2.963	4.010	14 points > 0
J-350	2.585	3.724	
J-341	2.538	4.285	
J-400	2.207	3.867	
J-318	1.181	2.137	
J-412	0.907	1.640	
J-408	0.673	1.359	
J-117	0.670	1.254	
J-410	0.601	0.977	
J-352	0.464	2.886	
J-395	0.248	0.762	
J-387	0.191	1.238	
J-345	0.148	0.303	
J-391	0.101	0.205	
J-385	0.058	0.780	
J-32	0.000	0.000	

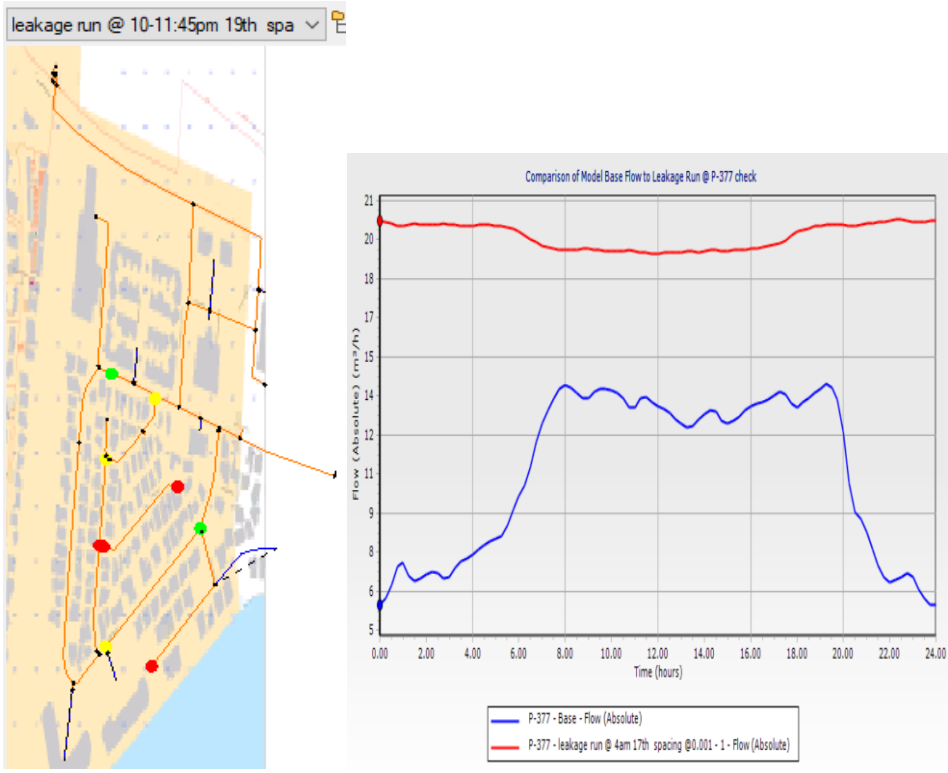

Figure 18: Graph showing Comparison of Model Base Flow to Leakage Run @ P-377 check on the 17th OCT 2021

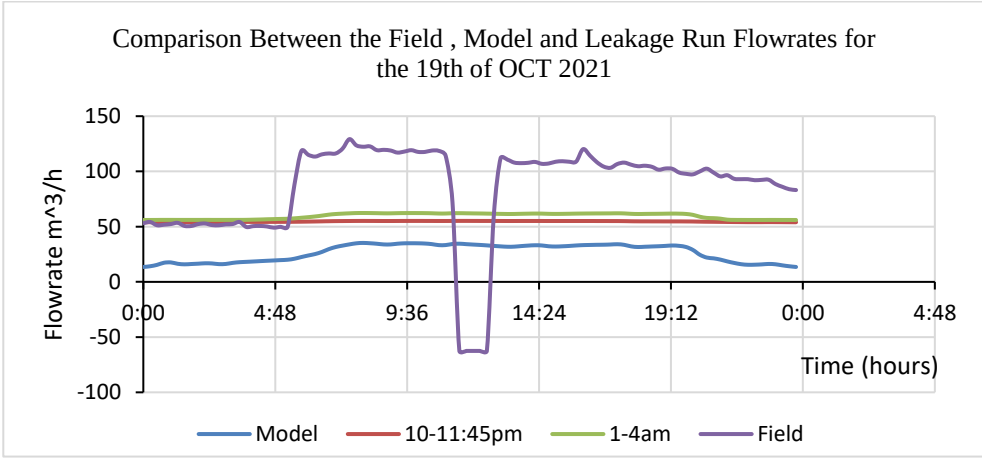

Figure 19: Graph showing the Comparison Between the leakage Runs, Base Model and Field Flowrates

DISCUSSION

Using WaterGEMS to determine the locations of leaks within a water distribution network will help modernize the Water and Sewage Authority. The software will allow the engineers within the organization to determine the general location and flow lost to the environment due to a leak within the multiple networks around the island. This discussion will analyze the data above, to determine the general locations of the leaks present within the West Moorings system. The field data was collected within the month of October 2021, so a field visit to prove the precision and accuracy of the software is impossible at this point.

As mentioned in the analysis the data obtained was color coded to easily identify the junctions with emitter coefficient values greater than 0, a range was also created to determine the junctions with the highest to lowest coefficients.

Emitter Coefficients

To obtain the data within the tables above we needed to determine a Emitter Coefficient range which allowed the Genetic Algorithm (Darwin Calibrator) to produce a model flowrate which is comparable to the actual flowrate on site. The software determined the flowrate of the model by using the Emitter Coefficient and the pressure head present at all the junction nodes using the equation $Q = KP^n$.

Comparison of Table 1 and 2 to identify the pros and cons of smaller Emitter Coefficient

We used the range of 0 to 3.6$\frac{\frac{m^3}{h}}{(m\ per\ H_2O)^n}$. These data sets were then used by Watergems to determine the junctions where leaks are present. NB: Within this discussion we look at the emitter coefficient values that are more than 0.72 $\frac{\frac{m^3}{h}}{(m\ per\ H_2O)^n}$.

Table 1 shows the 10 junctions identified to have a emitter coefficient > 0 at 2am on the 18th of OCT 2021. The emitter Coefficient spacing used was 0.036. While Table 2 shows data for the same period but a emitter coefficient spacing of 0.0036 Identified 15 junctions. With the smaller coefficient identifying more leakage nodes it was determined to be the better option.

The junctions identified with emitter coefficients mostly varied between both tables, but the general pattern showed that a leak was present on ocean boulevard between junctions J-332 and J-317. The data also showed large emitter values on the entirety of Santa Maria Avenue, Nina Drive and Columbus circle. Since the larger emitter coefficient provided less nodes to consider the precision in identifying the general area of a leak within the system using watergems was lower. They gave the same general locations of leaks on the system as the smaller locations, but it was unable to minimize the search area for the field

teams. This means that the on-site work in identifying the leak's exact location within the system will be greater than if the smaller coefficient is used.

Something to note, a greater density of junctions/ nodes within the model would be useful in identifying leaks since it will give the software more points of refence from which to base its calculations. The same with extra field data measured from multiple points on the field.

Why do we analyze multiple time periods?

The analysis above for the 18th of October 2021 was conducted within the early morning to ensure the data obtained from Watergems represented a system with low levels of usage. This means that the program will not misunderstand human daily usage as leaks within the system.

The analysis was conducted at 1am, 2am, 3am, 4am and between 1-4am to obtain 5 data sets to determine which period or individual interval gave an accurate leak location. Since the varies interval to interval we look at a set period between 1-4 am and 10-11:45 pm per day. This was done because the calibrator will focus on the recurring results within multiple individual intervals, discounting the ones it considers to be anomalies. These anomalies can be considered uncommon usage within the area like an overnight event within a resident's home or a 24hr business or even a illegal tap. This assumption was determined by looking at the model data at the times stated earlier in the paragraph.

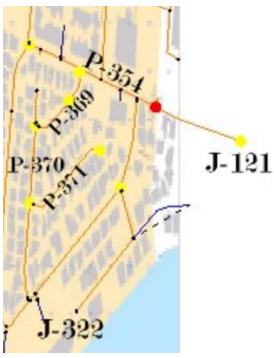

1am

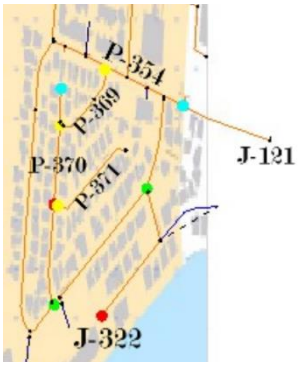

2am

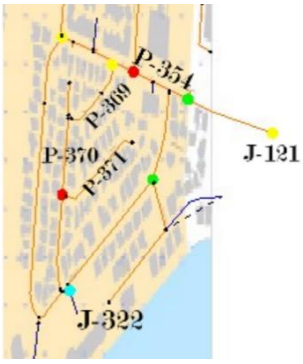

3am

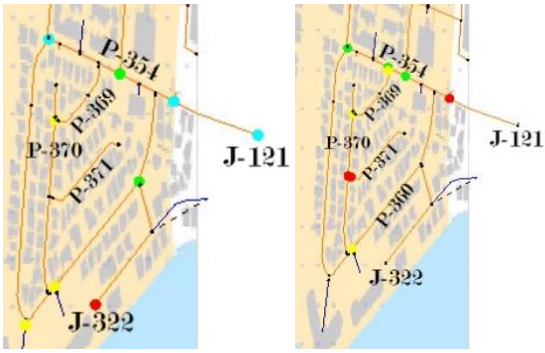

4am **1-4am**

Image6: Showing the time intervals looked at 1,2,3,4 and 1-4am.

By looking at a single time the Calibrator will not be able to determine if any of the identified leaks can be considered anomalies like uncommon usage or an illegal tap on the network. At the 1am, 3am and 4am periods J-121 was identified as a node with an emitter coefficient larger than 0.72, while at 2am it was less than 0.72. If the simulation is run only at 1 specific time the data's accuracy in terms of the entire measured period is low. This can be used to obtain the general situation within the area but is not recommended if the purpose of the test is to identify leakage nodes.

The 1-4 am data set however covers 1am to 4am at a 15-minute interval. By doing this watergems determined the most common leakage nodes as highlighted above. Notice that J-121 has an emitter coefficient less than 0.72. Therefore, it can be determined that previously identified leaks were anomalies caused by human usage either at massy stores or the residential homes. The data also provided a more accurate emitter coefficient value at each of the junctions, which was then used to determine the area where the largest leaks are present. This is seen in the 1-4 am image above. The image shows that the two junctions J-400 and J-350 on Nina Drive or P-369 have an emitter value between 2.88-2.16 and flowrate around 4 m^3/h. Also, Junctions J-334 and J-392 on Columbus Circle and Nina Drive, had the largest emitter coefficients at 3.05 and 2.96.

Validating the Model

As seen in graph 2 the highest point on the model curve is and the highest point on the field data curve is. To ensure that the data collected from the software is accurate the Darwin Calibrator needs to be ran to calibrate the model data to fit the field data. This is seen in graphs 11,14 and 17. But the model could not be properly validated since the entire network was not modeled due to the software issue with the student version. The leakage flowrate curve (ie, the calibrated model curve) was significantly less than the measured field data. This needs to be considered as a limitation due to the modelling issue experienced. Another limitation that caused the curve to not follow the trend of the field curve would be a lack of multiple field pressure and flowrate data sets from the field. However, this did not hinder us from showing how to analyze the data that is outputted

from this model. It is recommended that the entire system is modeled, and multiple field data sources is obtained to ensure that the output data obtained is accurate.

Leak Location Assumptions Due to the Map Data

Now we look at leakage identification and the assumptions that will be made in determining the general area of the leak using the data obtained from the calibrated Watergems model. Note that the leakage nodes identified are not the actual leak locations, they are just the points on the field and within the model where the software has observed consistent anomalies.

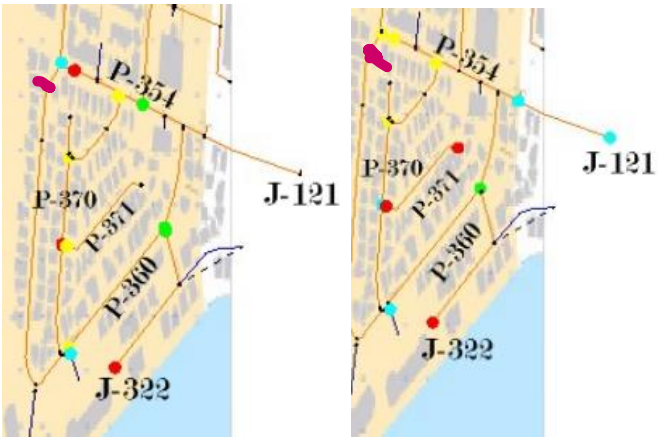

17th of October 2021

1-4am **10-11:45pm**

The pipe with the most leakage nodes is P-354. The area of the pipe that is highlighted by the purple line would be considered the area where the leak is mainly focused. Since at the morning period one of the leakage nodes was red and then within the evening period it turned to yellow. The value is still high but reduced due to a pressure change observed in the field data between the 1-4am and 10-12pm. In this situation the leak is assumed to be closer to the node highlighted red (J-412).

At P-371 the three junctions present emitter coefficient was all at red at some point on the 17th but changed color meaning the coefficient reduced throughout the day due to the pressure change between the 1-4am and 10-12pm period it can be assumed that a leak is present. The general location of the leak is nearer the left of P-371.

At P-369 at both times the emitter coefficient is constant therefore it is assumed a leak is present. It also means that the pressure and flowrate at this point is constant throughout the day or within the same allowable range. This is different to the above situations at P-371 and P-354.

At P-360 the emitter coefficients at the junctions are both low meaning that the size of the leak can assumed to be small. The leak is assumed to be closer to the J-387 (blue node), since it is the greater emitter coefficient.

At J-121 as mentioned in the above section is an anomaly and may not represent a leak but it may represent either an illegal tap or uncommon usage due to the location.

At J-322 the coefficient is constant throughout the measured periods. Therefore, it can be assumed there is a leak present near the node. The other nodes highlighted green J-318 and J-390 appear intermittently but the assumption can still be made that a leak is present within these sections.

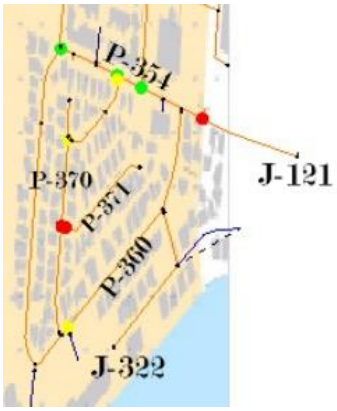

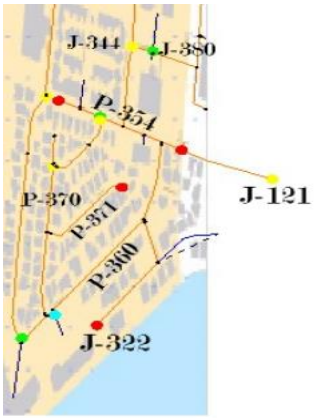

18th of October 2021

1-4am **10-11:45pm**

The situation on the 18th is similar to the 17th of October. The main differences would be the change in emitter coefficient values which is caused by the difference in flowrate and pressure that is present within the system.

At Junction J-380 and J-344 during the 10-11:45pm period an emitter coefficient is observed. This is different from the three previous periods checked. It can be assumed that this a leak or an unusual usage. Further checks will need to be conducted to determine if it is a leak or it is just an anomaly.

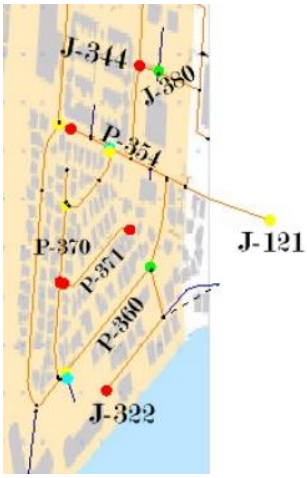

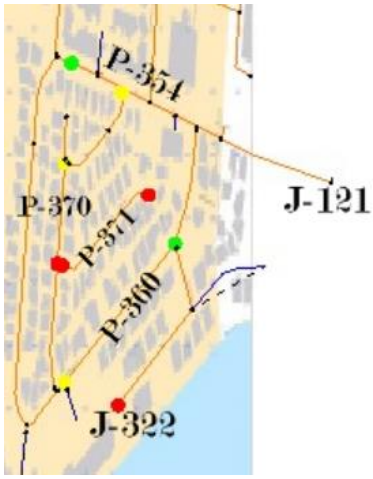

19th of October 2021

1-4am **10-11:45pm**

The situation for the 19th is the same as the two previous days so it can be assumed that the output from the software will be consistent for all the other days we have for measured field data.

The usage at J-380 and J-344 is present in the 1-4am period but not in the 10-11:45pm period therefore it can be determined that it was an anomaly and not a leak. The activity may be a resultant to an event at KFC or the Guardian Media Group Building.

The same can be said about J-121 and the junction before it, J-408. The emitter coefficients throughout the three days checked, continuously vary between the max range to the minimum range. This abnormal activity can be due to unauthorized usage by residents within the area.

How to use the findings?

One of the main objectives of this project is to identify leakage control methods to build resilience within the area of West Moorings. The data obtained can now be used to determine the best solution to solve the issues present and the exact location of the leak. We will recommend methods observed within the literature reviewed.

Since the leakage nodes with the largest emitter coefficients (3.6-2.88, red and yellow) were determined we now conduct a field visit to identify these leaks initially. As mentioned previously the exact Location of the leak cannot be determined within watergems. Alongside the watergems data, a field investigation using non-invasive methods like Ultrasonic leak detection and ground penetrating radar is necessary to determine the precise location of the leaks within the system. Ultrasonic leak detection uses a microphone which senses the sound waves that the water creates when it is exiting the orifice of the pipe. The sensor that the mic is attached to will determine the base frequency of the sound waves underneath the surface and once it comes above or within

range of the leak a notification will be displayed. The Ground Penetrating radar uses radio signals which it directs into the floor and the equipment will read the bounces that occur. These bounces will then be displayed as hyperbolas which, the technician will interpret to determine the leak depth and location. Then the normal repair practices can take place, that is either pipe replacement or pipe patching.

Once the largest leaks are dealt with, we then look at the smaller leaks within the system with the lowest emitter coefficient (less than 2.16, colors: blue, green and black). The damage caused to the environment from these leaks can be managed by reducing the operational pressure head and flowrate of the pumps on the network for a period. This method is a common practice but can cause a disturbance in supply so it should be used as a temporary measure and not permanent.

Anomalies within usage documented that is assumed to not be related to leaks. These anomalies need to be investigated to determine if it is related to illegal taps of the water supply.

RECOMMENDATIONS

By conducting this project many issues relating to information were identified. It was determined from the reviewed literature that watergems needs multiple different data sets throughout the network to accurately identify the locations of leaks within the network.

- If possible, model more junctions into the model to obtain more reference points for Watergems.
- Having at least 3 points with field data is necessary throughout a system. This provides the Darwin calibrator with a larger data base to simulate leaks with.
- Having real world demand data is also necessary since that data represents the actual demands of structures throughout the day.

LIMITATIONS

Throughout this project many limitations regarding data were experienced. To obtained accurate data within watergems the field data needs to also be accurate.

- The Student License for Bentley WaterGEMS has a limit on how many pipes that can be used therefore the individual chose the southeastern side of West Moorings to conduct the study. this affected the validity of the model.
- The water distribution network file was incomplete forcing the individual to assume the location of the pipes within that section of the network.
- Missing average demand data for certain commercial buildings forced the individual to use WASA average values to Calculate the demands.

- The Exact Location where the West Moorings DMA data was collected is unknown, so the location was assumed.

CONCLUSION

In Conclusion Watergems can be used to determine the general location of leaks within an existing distribution network. As mentioned in the above discussion the data obtained from watergems is not the exact therefore other methods leakage detection methods are needed when on site to determine the location of the leak. Since the parameters can be easily adjusted within watergems on site if the info shown is inaccurate it can be readjusted

Declaration of competing interest

The authors declare that they have no known competing financial interests or personal relationships that could have appeared to influence the work reported in this paper.

REFERENCES

AROUA N. (2022). Long term city development versus water strategy in Al-Maghreb, Larhyss Journal, No 50, pp. 173-197.

AROUA N. (2023). Setting out urban water issues, examples from Algeria and worldwide, Larhyss Journal, No 56, pp. 309-327.

AZADEH A., SALEHI V., ASHJARI B., SABERI M. (2013). Performance evaluation of integrated resilience engineering factors by data envelopment analysis: The case of a petrochemical plant, Science Direct, Vol. 92, Issue 3.

BAN F., ZHANG M., YE L. (2022). Water supply network modeling and pipe burst analysis based on WaterGEMS" School of Municipal and Environmental Engineering, Shenyang Jianzhu University, 110168 Liaoning, China.

BEKER B.A., KANSAL M.L. (2019). Evaluation of Municipal Water Distribution Using Water CAD and Watergems, Journal of Engineering and Sciences, Vol. 142.

BERREZEL Y.A., ABDELBAKI C., ROUISSAT B., BOUMAAZA T., KHALDOON A.M. (2023). Decision support system for the management of water distribution networks a case study of Tourville, Algeria, Larhyss Journal, No 54, pp. 7-24.

CAMPISANO A., MODICA C. (2015). Two-Step Numerical Method for Improved Calculation of Water Leakage by Water Distribution Network Solvers, ASCE Library, Vol. 142, Issue 2.

CHANNEL, Bentley Openflows For Water Infrastructure YT "WaterGEMS Advanced Part 14: Workshop 7, Leakage detection, 2019.

DERDOUR A., BELAM N., CHEBAB W. (2022). Traditional irrigation system and methods of water harvesting in the oasis of Sfissifa ksour mountains – Algeria, Larhyss Journal, No 49, pp. 17-35.

DESTA W.M., FEYESSA F.F., DEBELA S.K. (2022). Modeling and optimization of pressure and water age for evaluation of urban water distribution systems performance, Heliyon, Vol. 8, Issue 11.

DRINGOLI J. (2016). Options for modeling an outflow that varies with pressure, Bentley Communities.

FONTANA N., GIUGNI M., MARINI G. (2016). Experimental assessment of pressure-leakage relationship in a water distribution network, IWA Publishing, Water Science and Technology, Water Supply, Vol. 17, Issue 3.

HOUNTONDJI B., CODO F.P. (2019). Hydrogeological model for monitoring the drawdown of the groundwater of Monzoungoudo in Benin, Larhyss Journal, No 38, pp. 153-175.

IHSAN T., DEROSYA V. (2024). Drinking water problems in rural areas: review of point-of-use methods to improve water quality and public health, Larhyss Journal, No 58, pp. 55-71.

KEZZAR M.A., SOUAR A. (2024). The water management system in the village of Menades in Algeria-Between past and present, Larhyss Journal, No 57, pp. 55-79.

KOULOUGHLI C.E., TELLI A. (2023). Modern water supply management techniques and methods: a review, Larhyss Journal, No 55, pp. 7-23.

KOWALSKA B., SUCHORAB P., KOWALSKI D. (2022). Division of district metered areas (DMAs) in a part of water supply network using WaterGEMS (Bentley) software: a case study, Applied Water Science, Vol. 12.

MEHTA D., PRAJAPATI K., VERMA S., KUMAR V. (2024). Analysis of water distribution network using Epanet: a case study of Variav headwork Surat-India, Larhyss Journal, No 57, pp. 81-100.

MOHSENI U. (2022). Design and Analysis of Water Distribution Network Using Watergems, A Case Study of Narangi Village. In: Vasant, P., Zelinka, I., Weber, G.W. (Eds), Intelligent Computing & Optimization, ICO 2021, Lecture Notes in Networks and Systems, Springer, Vol. 371.

PANDEY P., MISHRA R., CHAUHAN R.K. (2022). Future prospects in the implementation of a real-time smart water supply management and water quality monitoring system, Larhyss Journal, No 51, pp. 237-252.

PATEL K., MEHTA D. (2022). Design of the continuous water supply system using Watergems software: a case study of Surat city, Larhyss Journal, No 50, pp. 125-136.

ROUISSAT B., SMAIL N. (2022). Contribution of water resource systems analysis for the dynamics of territorial rebalancing, case of Tafna system, Algeria, Larhyss Journal, No 50, pp. 69-94.

SALUNKE P.S., DUMANE M.M, KAMBLE S.P., NALVADE O.S., PONDKULE S.P., BINAYKE R.A. (2018). An Overview: Water Distribution Network by Using Water GEMS Software, Journal of Advances and Scholarly Researches in Allied Education, Vol. 15, Issue 2.

SHAHHOSSEINI A., NAJARCHI M., NAJAFIZADEH M.M., HEZAVEH M.M. (2023). Performance optimization of water distribution network using meta-heuristic algorithms from the perspective of leakage control and resiliency factor, case study: Tehran water distribution network, Iran, Science Direct, Vol. 20.

ŚWITNICKA K., SUCHORAB P., KOWALSKA B. (2017). The optimisation of a water distribution system using Bentley WaterGEMS software, ITM Web Conference, Vol.15.